OPEN

Cell Death and Differentiation (2013) 20, 953–962

www.nature.com/cdd

Genetic disruption of Abl nuclear import reduces renal apoptosis in a mouse model of cisplatin-induced nephrotoxicity

P Sridevi[1], MK Nhiayi[1] and JYJ Wang*[,1]

DNA damage activates nuclear Abl tyrosine kinase to stimulate intrinsic apoptosis in cancer cell lines and mouse embryonic stem cells. To examine the *in vivo* function of nuclear Abl in apoptosis, we generated *Abl-μNLS* (*μ, mutated in nuclear localization signals)* mice. We show here that cisplatin-induced apoptosis is defective in the renal proximal tubule cells (RPTC) from the $Abl^{\mu/\mu}$ mice. When injected with cisplatin, we found similar levels of platinum in the $Abl^{+/+}$ and the $Abl^{\mu/\mu}$ kidneys, as well as similar initial inductions of p53 and PUMAα expression. However, the accumulation of p53 and PUMAα could not be sustained in the $Abl^{\mu/\mu}$ kidneys, leading to reductions in renal apoptosis and tubule damage. Co-treatment of cisplatin with the Abl kinase inhibitor, imatinib, reduced the accumulation of p53 and PUMAα in the $Abl^{+/+}$ but not in the $Abl^{\mu/\mu}$ kidneys. The residual apoptosis in the $Abl^{\mu/\mu}$ mice was not further reduced in the $Abl^{\mu/\mu}; p53^{-/-}$ double-mutant mice, suggesting that nuclear Abl and p53 are epistatic to each other in this apoptosis response. Although apoptosis and tubule damage were reduced, cisplatin-induced increases in phospho-Stat-1 and blood urea nitrogen were similar between the $Abl^{+/+}$ and the $Abl^{\mu/\mu}$ kidneys, indicating that RPTC apoptosis is not the only factor in cisplatin-induced nephrotoxicity. These results provide *in vivo* evidence for the pro-apoptotic function of Abl, and show that its nuclear localization and tyrosine kinase activity are both required for the sustained expression of p53 and PUMAα in cisplatin-induced renal apoptosis.
Cell Death and Differentiation (2013) **20,** 953–962; doi:10.1038/cdd.2013.42; published online 10 May 2013

The ubiquitously expressed Abl tyrosine kinase contains three nuclear localization signals (NLS), a nuclear export signal (NES),[1,2] and undergoes nucleocytoplasmic shuttling in response to cell adhesion or DNA damage.[2] The cytoplasmic Abl is activated by growth factors, cytokines, extracellular matrix proteins, and microbial infections to regulate a wide variety of actin-based cellular processes.[3] The nuclear Abl is activated by DNA damage to regulate gene expression and DNA repair.[4,5] Previous cell-based studies have shown that DNA damage stimulates the nuclear accumulation and the activation of Abl tyrosine kinase through ATM and DNA-PK-dependent mechanisms,[6–8] and that Abl stimulates apoptosis by activating the p53-family of transcription factors.[9–12] Furthermore, nuclear entrapment can convert the oncogenic BCR-ABL tyrosine kinase into a death inducer.[13] The *in vivo* demonstration of the apoptosis function of Abl has been hampered by the neonatal lethality of the *Abl*-knockout mice.[14] The $Abl^{-/-}$ mice are runt and suffer from many developmental defects that make them unsuitable for the study of stress-induced cell death. We have shown that *Abl* knockout interferes with the neuronal apoptosis in the *Rb*-knockout embryos.[15] However, that result did not provide evidence for the pro-apoptotic function of Abl in DNA damage response. As DNA damage signaling is initiated in the nucleus, we generated the *Abl-μNLS* (*μ*; *mutated in the NLS*) allele by knockin substitution mutations of 11 Lys and Arg with Gln in the three NLS in the mouse *Abl1* gene[7] (Supplementary Figure s1). In embryonic stem (ES) cells, the *Abl-μNLS* mutation blocked nuclear import and reduced Bax activation by DNA damage.[7] We have since achieved germline transmission of the *Abl-μNLS* allele and show here that the $Abl^{\mu/\mu}$ mice are protected from cisplatin-induced renal apoptosis.

We chose cisplatin-induced nephrotoxicity as an experimental model because it is a toxic side effect in platinum-based therapies of ovarian, testicular, and other cancers.[16] The epithelial cells of the renal proximal tubules (RPTC) are particularly sensitive to cisplatin due to an active uptake mechanism, and these cells undergo cisplatin-induced apoptosis.[17,18] Previous studies using mouse genetic models have identified a number of mechanisms underlying cisplatin-induced nephrotoxicity, including intrinsic apoptosis, mitochondrial reactive oxygen species (ROS) production, and inflammation.[19–21] In this study, we provide evidence that the nuclear import and the tyrosine kinase activity of Abl are also required for cisplatin to induce RPTC apoptosis in the mice.

[1]Division of Hematology-Oncology, Department of Medicine, Moores UCSD Cancer Center, UCSD School of Medicine, University of California, San Diego, La Jolla, CA, USA

*Corresponding author: JYJ Wang, Division of Hematology-Oncology, Department of Medicine, Moores UCSD Cancer Center, School of Medicine, University of California,San Diego, 3855 Health Sciences Drive, Room 4328, La Jolla, CA 92093-0820, USA. Tel: 858 534 6253; Fax: 858 534 2821; E-mail: jywang@ucsd.edu
Keywords: nephrotoxicity; p53; proximal renal tubule cells; PUMA-α; tyrosine kinase

Abbreviations: AKI, acute kidney injury; ANOVA, analysis of variance; BUN, blood urea nitrogen; ES, embryonic stem; IHC, immunohistochemistry; LMB, leptomycin B; MEF, mouse embryo fibroblasts; MOMP, mitochondrial outer membrane permeabilization; NES, nuclear export signal; NLS, nuclear localization signal; PAS, Periodic Acid Schiff; PT, proximal tubule; ROS, reactive oxygen species; RPTC, renal proximal tubule cells; TKE, total kidney extracts; TUNEL, terminal deoxynucleotidyl-transferase dUTP nick end labeling; μNLS, mutated in nuclear localization signals

Received 13.10.12; revised 08.3.13; accepted 08.4.13; Edited by G Melino; published online 10.5.13

Results

RPTCs from $Abl^{\mu/\mu}$ mice are resistant to cisplatin-induced apoptosis. We succeeded in germline transmission of the *Abl-μNLS* allele (Supplementary Figure s1) and found that the $Abl^{\mu/\mu}$ mice are healthy and fertile (Table 1). In mice, the knockout of the Abl-related gene (*Arg/Abl2*) alone is well tolerated, but the combined loss of *Abl* and *Arg* caused early embryonic lethality.[22] We found that homozygous mutations of *Abl-μNLS* and *Arg* caused late embryonic lethality due to brain developmental defects, indicating that *Arg* is required for the proper development of the $Abl^{\mu/\mu}$ mice (not shown). Together, these breeding results show that nuclear Abl is not essential to mouse development, and that defect in the cytoplasmic Abl function causes neonatal lethality. In the $Abl^{\mu/\mu}$ mouse embryo fibroblasts (MEFs), only cytoplasmic Abl was detected (Figure 1a). Treatment with leptomycin B (LMB), which inhibits nuclear export,[2,7] caused Abl nuclear accumulation in the $Abl^{+/+}$ but not in the $Abl^{\mu/\mu}$ MEFs (Figure 1a). We also prepared primary cultures of RPTC (Figure 1b) and confirmed their identity by the expression of Megalin (Lrp2, an endocytosis receptor for protein reabsorption)[23] (Figure 1c). In the $Abl^{+/+}$ RPTC, Abl was diffusively localized in the cytoplasm and the nucleus, whereas only cytoplasmic Abl was detected in the $Abl^{\mu/\mu}$ RPTC (Figure 1d). Cisplatin treatment induced nuclear accumulation of Abl but not Abl-μNLS in the $Abl^{+/+}$ and the $Abl^{\mu/\mu}$ RPTC, respectively (Figure 1d). Cisplatin also induced DNA fragmentation in RPTC, and this response was reduced in the $Abl^{\mu/\mu}$ RPTC (Figure 1e). This result is consistent with the previous finding that cisplatin-induced apoptosis was reduced in the $Abl^{\mu/\mu}$ ES cells.[7]

Cisplatin-induced p53 response is blunted in $Abl^{\mu/\mu}$ kidneys. We then compared the *in vivo* apoptotic response in the $Abl^{+/+}$ and the $Abl^{\mu/\mu}$ kidneys in a model of cisplatin-induced nephrotoxicity.[24] We observed similar platinum levels in the $Abl^{+/+}$ and the $Abl^{\mu/\mu}$ kidneys at 24 and 48 h (Figure 2a), showing that the renal uptake, accumulation, and removal of platinum were not affected by the *Abl-μNLS* mutation. In both the $Abl^{+/+}$ and the $Abl^{\mu/\mu}$ mice, cisplatin injection induced nuclear p53 expression in the kidney tissues (Figures 2b and c). Nuclear p53 signal was not detectable in cisplatin-treated $p53^{-/-}$ mice, demonstrating specificity of this immunohistochemistry (IHC) assay (Figure 2b). At 30 h after cisplatin injection, we found similar numbers of nuclear p53-positive cells in the $Abl^{+/+}$ and $Abl^{\mu/\mu}$ renal tissues (Figure 2c, left). At this time point, co-injection with the Abl kinase inhibitor imatinib did not significantly alter the numbers of nuclear p53-positive cells in the $Abl^{+/+}$ or the $Abl^{\mu/\mu}$ renal tissues (Figure 2c, left). At 48 h after cisplatin injection, the number of nuclear p53-positive cells increased in the $Abl^{+/+}$ but not in the $Abl^{\mu/\mu}$ kidneys (Figure 2c, right). At the 48-h time point, co-injection with imatinib significantly reduced nuclear p53-positive cells in the $Abl^{+/+}$ but not in the $Abl^{\mu/\mu}$ kidney tissues (Figure 2c). The IHC results were confirmed by immunoblotting of total kidney extracts. The levels of p53 protein at 30 h after cisplatin injection were similar in the total extracts from the $Abl^{+/+}$ and the $Abl^{\mu/\mu}$ kidneys, but p53 protein levels were reduced by 48 h in the $Abl^{\mu/\mu}$ kidneys (Figure 2d, Supplementary Figure s2b). Co-injection with imatinib did not affect the p53 levels at 30 h in the $Abl^{+/+}$ or the $Abl^{\mu/\mu}$ kidneys (Figure 2d, left). However, co-injection with imatinib reduced the p53 levels in the $Abl^{+/+}$ but not in the $Abl^{\mu/\mu}$ kidneys at the 48-h time point (Figure 2d, right). We found that the *p53* mRNA was also upregulated in the $Abl^{+/+}$ and $Abl^{\mu/\mu}$ kidneys after cisplatin injection (Figure 2e). The induction of *Tp53* transcription could be due to the activation of protein kinase C-delta (PKCδ).[21,25] Interestingly, the *Tp53* mRNA levels were also reduced at the 48-h time point in the $Abl^{\mu/\mu}$ kidneys (Figure 2e). Taken together, these results show that the induction of p53 expression by cisplatin is not affected by the *Abl-μNLS* mutation. However, the continued accumulation of p53 in cisplatin-damaged renal tissues required the nuclear import and the kinase activity of Abl.

An important regulator of the p53 protein levels is the Mdm2 E3-ubiquitin ligase, which suppresses the accumulation of p53 at steady state.[26] In response to DNA damage, a number of pathways are activated to disrupt the p53-Mdm2 interaction, leading to the accumulation of p53.[27] The activated p53 then stimulates the transcription of Mdm2 to establish a negative feedback loop that controls the extent and duration of the p53 response.[28] We found similar basal levels of *Mdm2* mRNA in the untreated $Abl^{+/+}$ and the $Abl^{\mu/\mu}$ kidneys, and similar increases after cisplatin injection (Figure 2e). This result showed that nuclear Abl was not required for cisplatin to stimulate Mdm2 transcription. In total kidney extracts from the $Abl^{+/+}$ mice, the Mdm2 protein levels were elevated after cisplatin injection (Figure 2d, Supplementary Figure s2c). However, in the $Abl^{\mu/\mu}$ kidneys, the basal levels of Mdm2 protein were higher and cisplatin injection did not increase the Mdm2 protein despite upregulation of its mRNA (Figure 2d, Supplementary Figure s2c, Figure 2e). Treatment of mice with imatinib alone did not affect the basal levels of Mdm2 protein or mRNA in the $Abl^{+/+}$ or the $Abl^{\mu/\mu}$ kidneys (Figures 2d and e; Supplementary Figure s2c). Co-injection with cisplatin plus imatinib also had no effects on the Mdm2 mRNA (Figure 2e). However, co-injection with cisplatin plus imatinib caused reductions in Mdm2 protein in the $Abl^{+/+}$ and the $Abl^{\mu/\mu}$ kidneys (Figure 2d, Supplementary Figure s2c). A previous study showed that Mdm2-mediated p53 degradation could be inhibited by the ectopic expression of Abl or a kinase-defective Abl.[29] Furthermore, it was shown that Abl, but not Abl-μNLS, co-immunoprecipitated with Mdm2.[30] Those results suggest that the Abl–Mdm2 interaction would be lost in the $Abl^{\mu/\mu}$ mice, and this defect could have accounted for the blunted accumulation of the p53 protein in the $Abl^{\mu/\mu}$ kidneys. It has

Table 1 Genotypes of pups from breeding 10 pairs of $Abl^{+/\mu}$ heterozygous mice

Genotype[a]	No. of pups[b]	% expected frequency	% observed frequency
$Abl^{+/+}$	68	25	30.9
$Abl^{+/\mu}$	88	50	40.0
$Abl^{\mu/\mu}$	64	25	29.1

[a]Abl genotype, wild type (+), or *μNLS* (μ) was determined as described in Materials and Methods, and Supplementary Figure s1
[b]Total number of pups = 200; male = 115; female = 105

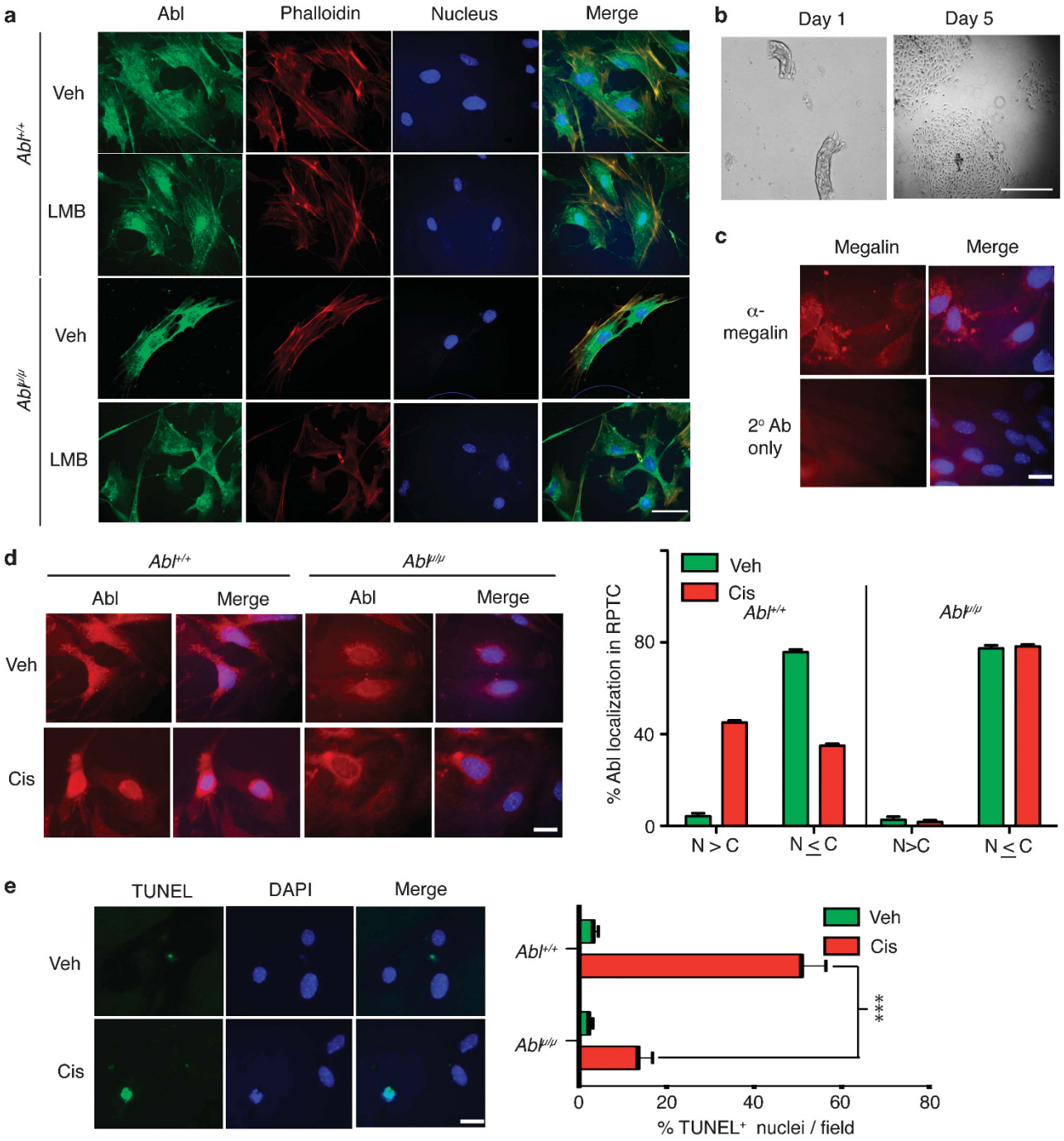

Figure 1 RPTCs from $Abl^{\mu/\mu}$ mice are resistant to cisplatin-induced apoptosis. (**a**) Fluorescence images of $Abl^{+/+}$ and $Abl^{\mu/\mu}$ mouse embryo fibroblasts treated with vehicle (Veh) or LMB (10 nM, 5 h) and stained for Abl (green), F-actin (phalloidin—TRITC, red), and DNA (blue). The scale bar is 25 μm. (**b**) Mouse RPTC in culture. Representative phase contrast micrographs of mouse RPTC at the indicated days in culture. The scale bar is 250 μm. (**c**) Immunofluorescence images of mouse RPTCs stained for Megalin (red) and DNA (blue). Scale bar = 25 μm. (**d**) Immunofluorescence images of RPTC of the indicated *Abl* genotypes fixed at 2 h after incubation with Veh or 20 μM cisplatin (Cis), and stained for Abl (red) and DNA (blue). Scale bar = 25 μm. Histogram shows quantification of subcellular Abl distribution in the indicated RPTC at 2 h. N > C is as depicted in the lower-left image panel in (**d**), the pattern of Abl distribution in the other three panels of (**d**) was scored as N ≤ C. Values shown are mean and S.D. from two independent experiments. (**e**) Quantification of TUNEL-positive RPTC of the indicated *Abl* genotypes fixed at 24 h after incubation with Veh or 10 μM Cis. Representative TUNEL-stained images of RPTCs are shown. DNA was stained with DAPI. Histogram shows mean and S.D. of percent TUNEL-positive nuclei (green) per field for the indicated genotypes and treatments. Between 200 and 300 nuclei were counted in at least six fields per genotype per treatment. Scale bar = 25 μM. ***represents $P = 0.0001$ by two-way analysis of variance (ANOVA)

also been reported that Abl can phosphorylate Mdm2 at Y-394.[30] However, because the kinase-defective Abl could stabilize p53,[29] pY394-Mdm2 is not likely to be required for Abl to stimulate p53 expression. Our finding that imatinib reduced Mdm2 protein in cisplatin-treated $Abl^{+/+}$ and in the $Abl^{\mu/\mu}$ kidneys indicates that the cytoplasmic Abl tyrosine kinase,

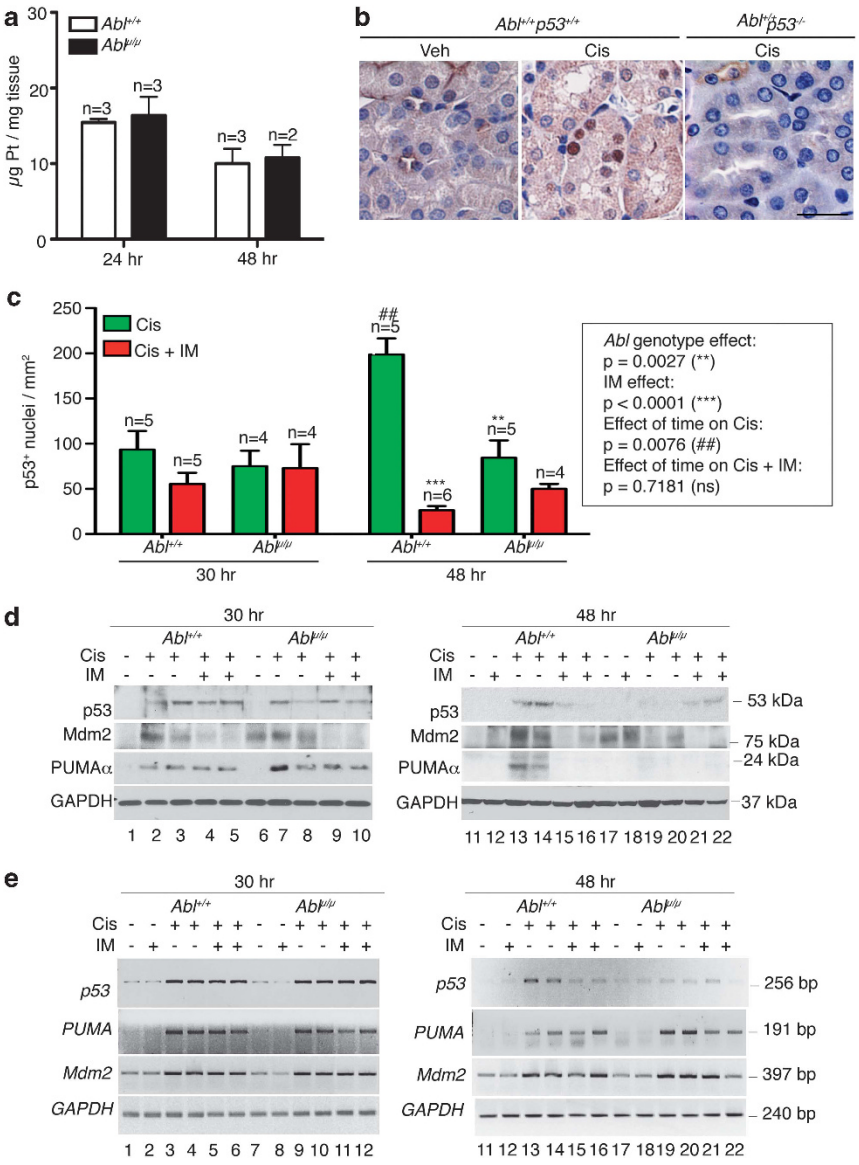

Figure 2 Cisplatin-induced p53 response is blunted in $Abl^{\mu/\mu}$ kidneys. (**a**) Kidney platinum levels were determined by ICP-MS, as described in Materials and Methods. The values shown are mean and S.D. from two independent experiments. *n* = number of mice per genotype. (**b**) Representative IHC images showing cisplatin-induced nuclear p53 expression. Scale bar = 100 μm. (**c**) Quantification of p53-positive nuclei at 30 and 48 h after cisplatin injection with or without imatinib (IM), as described in Materials and Methods. Values shown are mean and S.E.M. of p53-positive nuclei /mm^2, counted from eight, $\times$ 200 fields. Box next to the histogram shows statistical significance of the data determined by two-way ANOVA. (**d**) Levels of p53, PUMAα and Mdm2 protein in total kidney extracts (TKE) from the indicated mice at 30 h (left) or 48 h (right) after the indicated treatments. GAPDH: glyceraldehyde 3-phosphate dehydrogenase as loading control. Each lane contains the TKE from a different mouse. (**e**) Semi-quantitative RT-PCR of *p53*, *PUMA*, *Mdm2*, and *GAPDH* RNA in total kidney extracts from the indicated mice at 30 h (left) or 48 h (right) after the indicated treatments. Each number corresponds to total RNA sample from a different mouse

or another enzyme that is inhibited by imatinib, may regulate the expression of Mdm2 protein in response to DNA damage.

An important target gene of p53 in apoptosis is PUMAα.[31] At 30 h after cisplatin injection, similar levels of PUMAα induction were found in the $Abl^{+/+}$ and $Abl^{\mu/\mu}$ kidney extracts and tissues (Figure 2d; Supplementary Figures s2a and d). However, PUMAα levels were reduced in the $Abl^{\mu/\mu}$ kidney extracts and tissues by 48 h (Figure 2d; Supplementary Figures s2a and d). Imatinib co-treatment did not affect the levels of PUMAα at 30 h, but reduced its levels in the $Abl^{+/+}$ kidneys by 48 h (Figure 2d, right). We found that the *PUMA* RNA was similarly induced and maintained in the $Abl^{+/+}$ and the $Abl^{\mu/\mu}$ kidneys (Figure 2e). Furthermore, imatinib co-treatment did not affect the levels of *PUMA* RNA (Figure 2e). These results show that nuclear import of Abl and its kinase activity are not required for cisplatin to activate the transcription of the *PUMA* gene in the $p53^{+/+}$ genetic background. However, these results suggest that PUMAα protein expression could not be sustained despite the upregulation of its mRNA in the $Abl^{\mu/\mu}$ kidneys.

Reduction in apoptosis and proximal tubule damage in *Abl$^{\mu/\mu}$* kidneys. The expression of p53 and PUMAα did not cause DNA fragmentation assessed by TUNEL (terminal deoxynucleotidyl-transferase dUTP nick end labeling) staining. However, TUNEL-positive nuclei became detectable at 48 h (Figure 3a). In keeping with reduced apoptosis of the explanted RPTC (Figure 1e), the numbers of TUNEL-positive cells were significantly lower in the *Abl$^{\mu/\mu}$* than in the *Abl$^{+/+}$* kidneys (Figures 3a and b). Co-injection with imatinib reduced TUNEL-positive cells in the *Abl$^{+/+}$* but not in the *Abl$^{\mu/\mu}$* kidneys (Figures 3a and b). The reduced TUNEL staining correlated with the reduced expression of p53 and PUMAα in the *Abl$^{\mu/\mu}$* kidneys at the 48-h time point (Figure 2). At 72 h after cisplatin injection, TUNEL staining became unreliable due to the accumulation of protein casts in the renal tissues (Figure 3c). We therefore assessed the proximal tubule (PT) damage by PAS (Periodic Acid Schiff) staining, which reacts with the brush borders of PT epithelial cells and the glycoprotein aggregates (casts) that accumulate in the damaged PT.[32] In the *Abl$^{+/+}$* renal tissues, PAS-positive casts (*) and droplets (arrows) were readily detected at 72 h (Figures 3c and d); by comparison, these PAS-positive features were significantly lower in the *Abl$^{\mu/\mu}$* tissues (Figures 3c and d). Imatinib treatment alone did not alter the PAS staining or the PT morphology in renal tissues (Figures 3c and d). However, co-injection with cisplatin plus imatinib significantly reduced the number of PAS-positive protein casts in the *Abl$^{+/+}$* but not in the *Abl$^{\mu/\mu}$* kidneys (Figures 3c and d). These results showed that the reduced apoptosis (48 h) correlated with reduced PT damage (72 h) in the *Abl$^{\mu/\mu}$* kidneys. Therefore, cisplatin-induced renal apoptosis and PT damage require the nuclear import and the tyrosine kinase activity of Abl.

No further reduction of renal apoptosis by combining *Abl-μNLS* with *p53-null* mutations. It has been demonstrated that cisplatin-induced renal apoptosis requires p53.[33] We therefore compared the apoptotic response in the *Abl$^{\mu/\mu}$* and the *p53$^{-/-}$* kidneys. To compare littermates, we first generated the *Abl$^{+/\mu}$*; *p53$^{+/-}$* mice. Intercrossing of these compound heterozygotes generated *p53$^{-/-}$*; *Abl$^{\mu/\mu}$* male, but not female, pups at the expected Mendelian frequency (Table 2), indicating female-specific developmental defects of the double mutants. Interestingly, we found that the renal apoptotic response to cisplatin was reduced to similar low levels in the *Abl$^{\mu/\mu}$* and the *p53$^{-/-}$* single-mutant mice (Figure 4c). These lower levels of TUNEL staining were not further reduced in the *Abl$^{\mu/\mu}$; p53$^{-/-}$* double-mutant kidneys

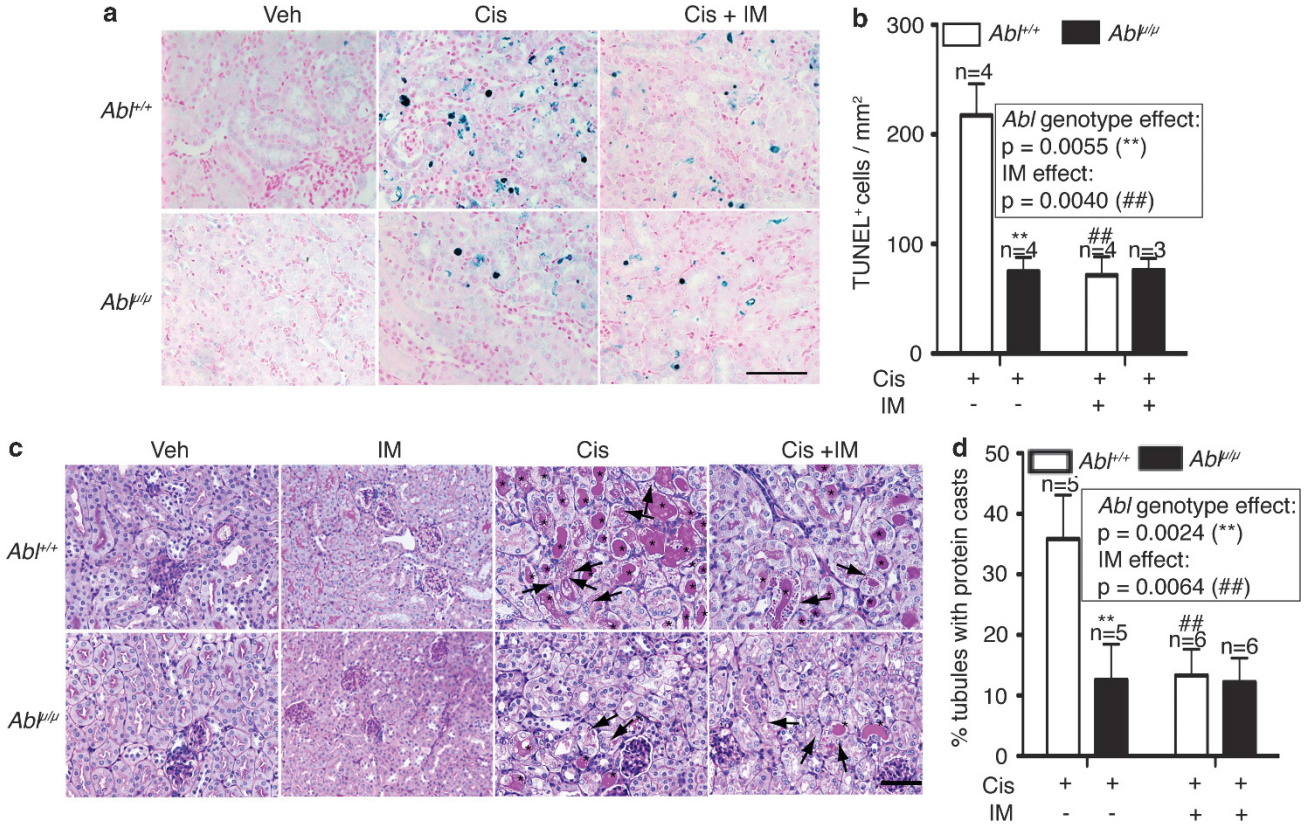

Figure 3 Reduction in apoptosis and proximal tubule damage in *Abl$^{\mu/\mu}$* kidneys. (**a**) Representative TUNEL staining of kidney tissue sections of mice of the indicated genotypes at 48 h after the indicated treatments. Scale bar = 100 μm. (**b**) Quantification of TUNEL-positive cells. Values shown are mean and S.E.M. of TUNEL-positive cells / mm^2, counted from eight, × 200 fields, for each mouse. *n* = number of mice per treatment per genotype. Inset shows statistical significance determined by two-way ANOVA. (**c**) Representative images of PAS-stained kidney sections from mice of the indicated *Abl* genotypes killed at 72 h after the indicated treatments. Scale bar = 100 μm. * indicates PAS-positive casts and arrows point to PAS-positive droplets. (**d**) Quantification of PAS-positive casts. Values shown are mean and S.E.M. of % tubules with PAS-positive casts from eight fields per animal. *n* = number of animals per treatment per genotype. Inset shows statistical significance determined by two-way ANOVA

(Figures 4a and c). We also measured PT damage by PAS staining at 72 h and found that the levels of cast-positive tubules were similarly reduced in each of the single- and the double-mutant kidneys (Figures 4b and d). Moreover, there were no significant differences among the *Abl*$^{\mu/\mu}$*; p53*$^{+/+}$, the *Abl*$^{+/+}$*; p53*$^{-/-}$, and the *Abl*$^{\mu/\mu}$*; p53*$^{-/-}$ kidneys in cisplatin-induced PT damage (Figures 4b and d). These results show that the nuclear Abl is as important as p53 in cisplatin-induced renal apoptosis and tubule damage, and that the nuclear Abl and p53 are epistatic to each other in this apoptotic response.

We also examined the levels of p53, PUMAα, and cleaved caspase-3 (ΔC3) in total kidney extracts from the single and the double mutants at the 72-h time point (Figure 4e, Supplementary Figures s3a–c). In the *Abl*$^{\mu/\mu}$*; p53*$^{+/+}$ kidneys, we observed variable, but consistent, reductions in p53, PUMAα, and ΔC3. In the *Abl*$^{+/+}$*; p53*$^{-/-}$ kidneys, we found reduced ΔC3 in kidneys with high levels of PUMAα in some mice (Figure 4e, Supplementary Figures s3b and c). Although *PUMA* was identified as a target gene of p53,[31] the transcription of *PUMA* can be stimulated by other factors including p63, p73, NF-kB, FOXO, and SMAD4.[34–38] Previous studies have shown that cisplatin activates the Abl tyrosine kinase to stimulate p63 and p73.[9–12] The wild-type level of PUMAα expression in some of the *Abl*$^{+/+}$*; p53*$^{-/-}$ kidneys could, therefore, be driven by the Abl-p63 or the Abl-p73 pathways. Previous studies have also shown that the cytoplasmic p53 can stimulate mitochondrial outer membrane permeability transition.[39–41] The loss of this cytoplasmic p53 function might explain the reduced ΔC3 formation in those *Abl*$^{+/+}$*; p53*$^{-/-}$ kidneys that expressed wild-type levels of PUMAα. In other words, both the PUMAα and the cytoplasmic p53 are required for cisplatin to induce caspase-3 cleavage in the mouse kidneys.[39–41] In the kidneys of the *Abl*$^{\mu/\mu}$*; p53*$^{-/-}$ double mutants, PUMAα and ΔC3 were further reduced (Figure 4e, Supplementary Figure s3b and c), consistent with the epistatic interaction of nuclear Abl and p53 in cisplatin-induced renal apoptosis. This result also indicated that other caspase-independent pathways[42] might account for the residual TUNEL positivity in the double-mutant kidneys.

Table 2 Genotypes of pups from breeding 40 pairs of *Abl*$^{+/\mu}$*p53*$^{+/-}$ compound heterozygous mice

Genotype[a]	No. of pups[b]	% expected frequency	% observed frequency	Male to female ratio
Abl$^{+/+}$*p53*$^{+/+}$	62	6.25	9.2	1.3
Abl$^{+/\mu}$*p53*$^{+/+}$	99	12.5	14.6	1.1
Abl$^{\mu/\mu}$*p53*$^{+/+}$	60	6.25	8.9	1.1
Abl$^{+/+}$*p53*$^{+/-}$	96	12.5	14.2	0.9
Abl$^{+/\mu}$*p53*$^{+/-}$	181	25	26.7	1.0
Abl$^{\mu/\mu}$*p53*$^{+/-}$	71	12.5	10.5	1.8
Abl$^{+/+}$*p53*$^{-/-}$	35	6.25	5.2	1.7
Abl$^{+/\mu}$*p53*$^{-/-}$	49	12.5	7.2	2.1
Abl$^{\mu/\mu}$*p53*$^{-/-}$	24	6.25	3.5	5.0

[a]Abl genotype: wild type (+) or μ*NLS* (μ); p53 genotype: wild type (+) or null (−), was determined as described in Materials and Methods, and Supplementary Figure s1
[b]Total number of pups = 677; male = 376; female = 301

Reduction in renal apoptosis did not ameliorate nephrotoxicity. In patients, nephrotoxicity is routinely assessed by blood urea nitrogen (BUN) and serum creatinine, which are delayed biomarkers for kidney injury, as these levels reflect the glomerular filtration rate.[43,44] Consistent with it being a delayed marker, we detected significant increases in the BUN levels only at the 72-h time point (Supplementary Figure s4a). We then measured the BUN levels across the nine genotypes generated by crossing the *Abl*$^{+/\mu}$*; p53*$^{+/-}$ mice, and found that BUN increases in all mice (Figure 5a). The variations in the BUN increases were statistically insignificant (Figure 5a). The serum-creatinine levels were also similarly increased between the *Abl*$^{+/+}$ and the *Abl*$^{\mu/\mu}$ mice (Supplementary Figure s4b). At a lower dose of cisplatin, the increases in BUN were again found to be similar between the *Abl*$^{+/+}$ and the *Abl*$^{\mu/\mu}$ mice (Supplementary Figure s4c). These results suggest that the kidneys were still injured in the *Abl*$^{\mu/\mu}$ mice. We therefore measured the levels of *Kim-1* (Kidney Injury Molecule-1) RNA, which is consistently upregulated in different models of kidney injury[44,45] and found similar levels of *Kim-1* induction by cisplatin in the *Abl*$^{+/+}$ and *Abl*$^{\mu/\mu}$ kidneys (Supplementary Figure s4d).

A recent study has shown that cisplatin activates Stat-1 phosphorylation in the cochlea of rats and that administration of Stat-1-siRNA blocked cisplatin-induced hearing loss measured by the auditory brainstem response threshold.[46] The phosphorylation of Stat-1 leads to activation of downstream targets such as iNos and Cox-2, which induce inflammation to cause hair cell damage.[46] We found that Stat-1 was expressed at comparable levels in the *Abl*$^{+/+}$ and the *Abl*$^{\mu/\mu}$ kidneys (Figure 5b). Injection with cisplatin stimulated Stat-1 phosphorylation to a low level at 30 h and a higher level at 48 h; and the increases in phosphor-Stat-1 (pStat1) were similar between the *Abl*$^{+/+}$ and *Abl*$^{\mu/\mu}$ kidneys (Figure 5b). Furthermore, co-injection with imatinib did not affect the increase in pStat1 in the *Abl*$^{+/+}$ or the *Abl*$^{\mu/\mu}$ kidneys (Figure 5b). These results show that cisplatin-induced Stat-1 phosphorylation was similarly upregulated in the *Abl*$^{+/+}$ and the *Abl*$^{\mu/\mu}$ kidneys. The pStat1 and possibly other cisplatin-activated pathways could explain the kidney injury detected in the apoptosis-defective *Abl*$^{\mu/\mu}$ mice (Figure 5c).

Discussion

The study of the *Abl-*μ*NLS* mice has provided the first *in vivo* evidence for the pro-apoptotic function of Abl, and shown that nuclear Abl is as important as p53 in cisplatin-induced renal apoptosis. Furthermore, this *in vivo* study has generated new insights on the nuclear Abl tyrosine kinase function in apoptosis. First, our previous study of the *Abl*$^{\mu/\mu}$ ES cells[7] and this study of the *Abl*$^{\mu/\mu}$ kidneys have shown that the induction of p53 expression by cisplatin does not require Abl nuclear import. Instead, we found that nuclear Abl is required for the continued accumulation of p53. Second, the study of the *Abl*$^{\mu/\mu}$ kidneys has indicated an unexpected role for nuclear Abl in the regulation of Mdm2 protein expression. Third, we have found that nuclear Abl is required for the sustained expression of PUMAα protein in cisplatin-induced apoptosis.

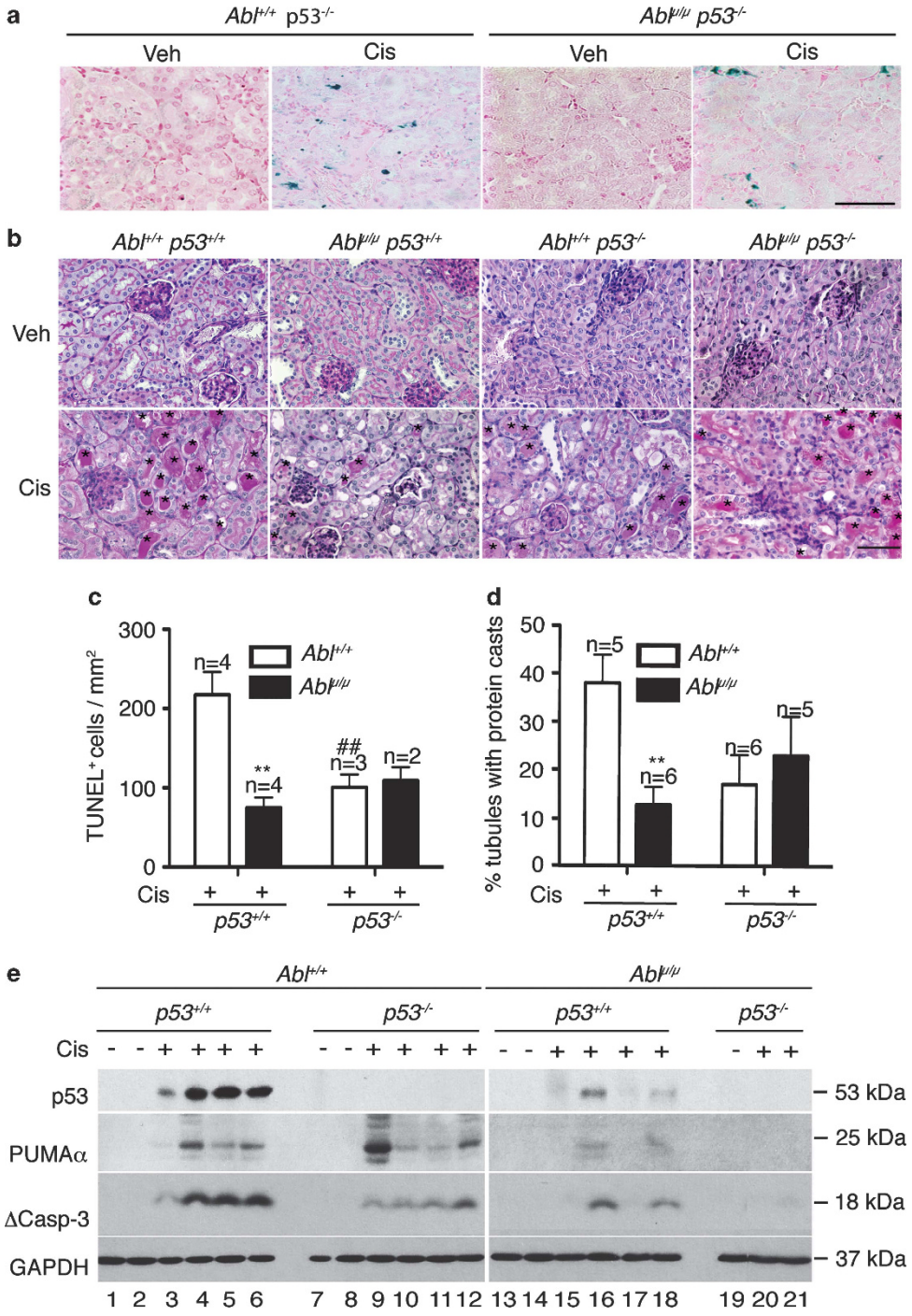

Figure 4 No further reduction of renal apoptosis by combining *Abl-μNLS* with *p53-null* mutations. (**a**) Representative TUNEL staining of kidney tissue sections of mice of the indicated genotypes at 48 h after cisplatin treatments. Scale bar = 100 μm. (**b**) Representative images of PAS-stained kidney sections from mice of the indicated genotypes killed at 72 h after the indicated treatments. Scale bar = 100 μm. * indicates PAS-positive casts and arrows point to PAS-positive droplets. (**c**) Quantification of TUNEL-positive cells. Values shown are mean and S.E.M. of TUNEL-positive cells /mm^2, counted from eight, × 200 fields, for each mouse. *n* = number of mice per treatment per genotype. ** p = 0.0055, ## p = 0.0085 by 2-way ANOVA. (**d**) Quantification of PAS-positive casts. Values shown are mean and S.E.M. of % tubules with PAS-positive casts from eight fields per animal. *n* = number of animals per treatment per genotype. ** p = 0.0024 by 2-way ANOVA. (**e**) Levels of p53, PUMAα, and cleaved caspase-3 (ΔCasp3) protein in TKE from the indicated mice at 72 h after cisplatin injection. GAPDH was used as loading control. Number below each lane represents lysate from a single mouse

The nuclear Abl-dependent p53 accumulation is consistent with the previous findings that Abl interacts with Mdm2 to block p53 degradation[29] and that the Abl-μNLS mutant protein is defective in binding Mdm2.[30] Besides the p53 protein, we found that its mRNA was also upregulated by cisplatin in the kidneys. A previous study has shown that DNA damage upregulates *Tp53* transcription through PKCδ,[25] which is activated by cisplatin in the mouse

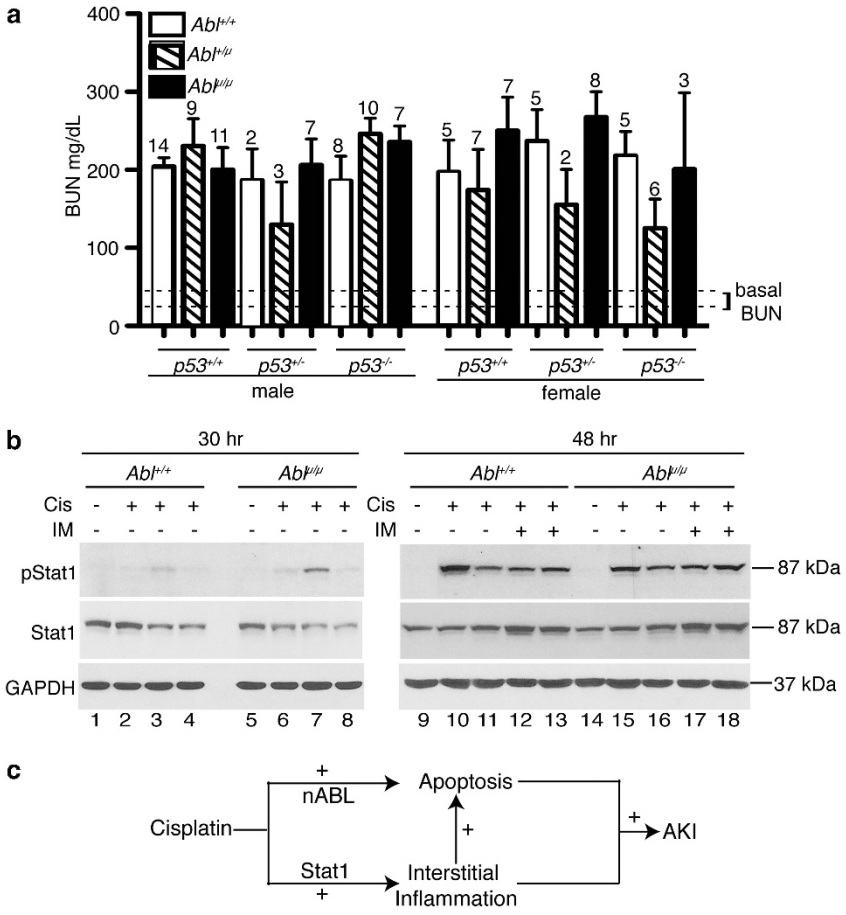

Figure 5 Reduction in renal apoptosis did not ameliorate nephrotoxicity. (**a**) BUN levels from mice of the indicated *Abl* and *p53* genotypes killed at 72 h of the indicated treatments. The mean and S.E.M. of BUN values, measured in duplicates per mouse, are shown. The number above each column indicates the number of mice per treatment. Dotted lines across the bottom of the columns indicate the range in which the BUN values of the untreated mice of the different genotypes fall. (**b**) Levels of pStat1 and Stat-1 protein in TKE from the indicated mice at 30 h (left) or 48 h (right) after the indicated treatments. GAPDH was used as loading control. Each lane contains the TKE from a different mouse. (**c**) Schematic showing role of nuclear Abl in cisplatin-induced acute kidney injury (AKI). Cisplatin activates nuclear Abl (nAbl) to stimulate renal apoptosis. Cisplatin also activates the Stat-1 pathway to stimulate kidney interstitial inflammation, which can further enhance renal apoptosis. A combination of renal apoptosis, interstitial inflammation, and other cisplatin-activated pathways lead to AKI

kidneys.[21] Several studies have suggested an interdependent activation of Abl and PCKδ by ROS.[47,48] Although the initial upregulation of the *Tp53* mRNA was not affected by *Abl-μNLS*, its levels were reduced at a later time, indicating that the PKCδ activity might be lowered in the $Abl^{\mu/\mu}$ kidneys.

An important pro-apoptotic target gene of p53 is PUMAα,[31,49] which is a BH3-only protein that sequesters the anti-apoptotic Bcl2-family members to stimulate Bax and Bak-dependent mitochondrial outer membrane permeabilization (MOMP).[50–54] We show here that nuclear Abl is not required for cisplatin to induce *PUMA*α RNA. However, nuclear Abl is required for the sustained expression of the PUMAα protein. This finding is completely unexpected and indicates a novel function for nuclear Abl in the regulation of PUMAα translation or protein stability. Interestingly, we found that cisplatin could still induce PUMAα expression in the $Abl^{+/+}; p53^{-/-}$ kidneys, but PUMAα expression was lost in the kidneys of the double-mutant mice ($Abl^{\mu/\mu}; p53^{-/-}$). The upregulation of PUMAα in the $Abl^{+/+}; p53^{-/-}$ mice is likely to be mediated by p63 and/or p73, as previous studies have established a redundant role of these three transcription factors in PUMAα expression.[34–38]

This study also shows that p53 and nuclear Abl-dependent apoptotic response is not the only factor in cisplatin-induced nephrotoxicity. The pathophysiology of acute kidney injury involves epithelial cell death, interstitial inflammation, small vessel obstruction, and local ischemia.[44] Other than apoptosis, cisplatin also induces oxidative stress, necrosis, autophagy, and inflammation in the renal tissues.[20,55] In the $Abl^{\mu/\mu}$ mice, injection with cisplatin stimulated the expression of Kim-1, which encodes a transmembrane glycoprotein that is upregulated in response to kidney injury caused by many different agents.[44,45] Furthermore, we found that cisplatin induced the phosphorylation of Stat-1 in the kidneys of the $Abl^{+/+}$ and $Abl^{\mu/\mu}$ mice. As Stat-1 has been shown to be required for cisplatin to cause ototoxicity (hearing loss) in the rats,[46] the activation of Stat-1 could have contributed to cisplatin-induced nephrotoxicity in the $Abl^{\mu/\mu}$ mice. Therefore, a concerted strategy that targets the nuclear Abl and the Stat-1 pathways may be required to ameliorate nephrotoxicity associated with platinum-based cancer therapy.

Materials and Methods

Materials. Pharmacological hospital-grade cisplatin (1 mg/ml in saline) was from APP Pharmaceuticals (Schaumburg, IL, USA). Imatinib mesylate, rabbit anti-p53 antibody (IHC and western blotting), goat anti-PUMAα antibody (IHC and western) were from Santa Cruz Biochemicals (Santa Cruz, CA, USA). Mdm2 antibody was from Calbiochem (EMD Millipore Biosciences, Billerica, MA, USA); pSTAT1 (Tyr701) antibody was from Cell Signaling Technology Inc. (Danvers, MA, USA); and STAT-1 antibody was from BD Biosciences (San Jose, CA, USA). Type-2 Collagenase, L-glutamine, nonessential amino acids, and DMEM F12 media were from Invitrogen (Carlsbad, CA, USA). Soybean trypsin inhibitor and hydrocortisone were from Sigma Aldrich (St Louis, MO, USA). Dextrose, glycine, 70-μ mesh cell culture sieve and fetal bovine serum (FBS) were from Fisher Scientific (Pittsbrugh, PA, USA). HBSS, Insulin Transferrin Selenium (ITS), and sodium pyruvate were from Cellgro (Manassas, VA, USA). Penicillin-streptomycin stock solution and Fungizone were from Mediatech (Manassas, VA, USA).

Genotyping primers. The *Abl* genotypes were determined from tail DNA by PCR using the following primers: forward, 5′-TGTGTCGACCCTCGGTGTCAT-3′, reverse, 5′-GATGGCCTCGAGAAAACTTCA-3′ (Supplementary Figure s1). Genotyping of the *p53-null* allele was according to Jacks *et al.*[56]

Mice. Breeding, handling, and experimentation with mice were according to protocols approved by The Institutional Animal Care and Use Committees of University of California at San Diego. Embryonic stem cells with one *AblμNLS (μ)* allele containing the neomycin-resistant gene (*neo*) cassette flanked by *loxp* sites were previously described.[7] Following germline transmission of this *Ablμ-loxP-Neo-loxP* allele, female were bred with male *protamine-Cre*-transgenic mice to remove the *Neo* cassette. The $Abl^{+/\mu}$ mice were then bred with the $p53^{+/-}$ mice (from the Jax lab, Bar Harbor, ME, USA) to generate a breeding colony of $Abl^{+/\mu}p53^{+/-}$ mice.

Cisplatin treatment. To induce acute renal failure, mice (8–10 weeks of age) were given a single intraperitoneal injection of cisplatin at 20 mg/kg body weight (b.w.). With imatinib treatment (50 mg/kg b.w.), mice were injected intraperitoneally with 2 mg/ml imatinib mesylate solution in PBS. Imatinib was given 2 h prior to cisplatin and every 12 h thereafter until the end of treatment. At this dose, the plasma concentration of imatinib is at 8–10 μM at 2 h after injection and decays thereafter, but remains above 1 μM for 8 h.[57] Mice were euthanized at the indicated time points by carbon dioxide asphyxiation; tissues were retrieved and blood collected by cardiac puncture.

Preparation of mouse RPTCs. Mouse RPTC were prepared as described.[58] Briefly, mouse renal cortices were minced in ice-cold dissection solution (10 mM glucose, 5 mM glycine, 1 mM alanine, 15 mM HEPES, pH 7.4, 150 mM NaCl with osmolality at 325 osmol/kg H_2O), digested for 30 min at 37 °C with type-2 collagenase (0.1% w/v in DS) and filtered through 70 μm mesh sieves. The PT fragments that did not pass through the 70-μm sieves were resuspended by flushing the sieve in the reverse direction with warm DS (37 °C) containing 1% (w/v) bovine serum albumin (BSA). The PT fragments were then cultured at 37 °C with 5% CO_2 in medium containing 1 : 1 DMEM/F12, 1% FCS, 15 mM HEPES, 2 mM L-glutamine, 50 nM hydrocortisone, 5 μg/ml each of insulin and transferrin, 50 nM selenium, 0.55 mM sodium pyruvate, nonessential amino acids, penicillin 100 IU/ml, and streptomycin 100 μg/ml, pH 7.4. The medium was changed every 2 days. For immunofluorescence staining, RPTC were directly seeded onto acid-washed and poly-L-lysine-coated coverslips. The percentage of RPTC in these primary cultures was $>80\%$, as determined by immunofluorescence staining for the RPTC marker megalin.

Immunofluorescence. Cells were fixed with 4% paraformaldehyde for 20 min, permeabilized with 0.3% Triton X-100 for 20 min, and blocked with 5% BSA for 30 min. The coverslips were incubated with anti-Abl (8E9) antibody (30 μg/ml) for 2 h, followed by ALEXA fluor-488 (Invitrogen)-chicken anti-mouse (1 : 500) for an hour at 37 °C. Nuclei were stained with DAPI (4′,6-diamidino-2-phenylindole dihydrochloride) (Sigma Aldrich).

Immunoblotting. Mouse kidneys were homogenized on ice in RIPA buffer (25 mM Tris-HCl pH 7.4, 1 mM EDTA, 0.1% SDS, 150 mM NaCl, 1% NP-40, 1% sodium deoxycholate, 1 mM phenylmethylsulfonyl fluoride, and protease inhibitor cocktail). The lysates were sonicated and centrifuged at 12 000 r.p.m. for 10 min. The supernatant was quantified using Bio-Rad Lowry protein assay reagent, and 30–50 μg lysates were loaded per lane of SDS polyacrylamide gels. Western blotting was performed by standard protocols.

RNA analysis. Total RNA was extracted from frozen kidneys using RNA extraction kit (Qiagen, Germantown, MD, USA) and converted to cDNA using ABI kit, following the manufacturer's protocol (Life Technologies, Carlsbad, CA, USA). The primer sets used were as follows: *GAPDH* (forward: 5′-TGATGACATCAA GAAGGTGGTGAAG-3′; reverse: 5′-TCCTTGGAGGCCATGTAGGCCAT-3′), *p53* exon 3 (forward: 5′-ACCTCACTGCATGGACGATCTG-3′; reverse: 5′-CGTGCA CATAACAGACTTGGC-3′), *PUMA* exon 3 (forward: 5′-CCTCAGCCCTCCCTGT CACCAG-3′; reverse: 5′-CAACGCGCAGTACGAGCGGCGG-3′), *Mdm2* exon 10 (forward: 5′-CATGCAATGAAATGAATCCTCCCC-3′; reverse: 5′- AATGCCATC GAACCATGTGT-3′), *KIM-1* exon 2 (forward: 5′ AATGCCATCGAACCATGTGT-3′; reverse: 5′- CCTTGACGATAGAGAACTCTGTTGAGA-3′). Total RNA without reverse transcription was used as control to rule out genomic DNA PCR.

Histology and IHC. For assessment of kidney tissue injury, 5-μm sections were stained with PAS. Tubular protein casts were counted in at least eight random fields in the PAS-stained sections. For p53 and PUMAα IHC, sections were deparaffinized, rehydrated, and antigen retrieval achieved by heating in Retrievagen A (pH 6.0) from BD biosciences, at 95 °C for 15 min. The sections were allowed to cool down, and immunostaining was performed using Dako DAB-IHC kit (Dako Technologies, Carpinteria, CA, USA), following the manufacturer's protocol to stain the antigen brown. Hematoxylin was used to counterstain the nuclei blue.

BUN and serum-creatinine measurement. Nephrotoxicity was assessed by BUN and serum creatinine levels using Quantichrom DI-UR500 urea assay kit and Quantichrom CT500 creatinine assay kit, respectively (Bioassay Systems, Hayward, CA, USA).

TUNEL assay. TUNEL was performed on tissue sections using Trevigen TACS.XL–Blue *in situ* apoptosis detection kit (Trevigen, Gaithersburg, MD, USA). Nuclei were counterstained with nuclear fast red. Sections were photographed ($\times$ 200), and apoptotic nuclei and apoptotic bodies in at least eight representative fields were counted per mouse. TUNEL labeling was performed on RPTC cells using Takara *In situ* Apoptosis Detection Kit. RPTC nuclei were stained with DAPI, and TUNEL-positive cells were counted in six fields out of a total of around 200 nuclei.

Measurement of tissue platinum. Whole kidneys were blotted dry, weighed, finely minced, transferred into conical tubes containing 215 μl of concentrated nitric acid, and digested overnight at 60 °C. The digested tissues were diluted with 3 ml of buffer containing 0.1% Triton X-100, 1.4% v/v concentrated nitric acid and 1 ppb Indium. The digested samples were subjected to inductively coupled plasma/mass spectroscopy (ICP-MS) to determine the platinum content.

Statistical methods. For statistical analysis, Prism 5.0 software (GraphPad Software, San Diego, CA, USA) was used. The statistical significance, when only two groups were compared, was assessed using *t*-test. Two-way ANOVA with Bonferroni post-test analysis was used to compare the effects of the different treatments (cisplatin *versus* cisplatin + IM) on the two *Abl* genotypes.

Conflict of Interest

The authors declare no conflict of interest.

Acknowledgements. We thank Preston Adams in the laboratory of Dr. Steve Howell at the Moores Cancer Center for assistance in the ICP-MS analysis of tissue platinum levels, the Histology shared facility of the Moores Cancer Center for paraffin embedding, tissue sectioning, and PAS staining, and Hung Nguyen for genotyping the mice. This work is supported by pilot funding from the UCSD NIH CTSA grant (5UL1TR000100) and a grant (RO1CA043054) from the National Cancer Institute to JYJW.

1. Wen ST, Jackson PK, Van Etten RA. The cytostatic function of c-Abl is controlled by multiple nuclear localization signals and requires the p53 and Rb tumor suppressor gene products. *EMBO J* 1996; **15**: 1583–1595.

2. Taagepera S, McDonald D, Loeb JE, Whitaker LL, McElroy AK, Wang JY *et al.* Nuclear-cytoplasmic shuttling of C-ABL tyrosine kinase. *Proc Natl Acad Sci USA* 1998; **95**: 7457–7462.
3. Woodring PJ, Hunter T, Wang JY. Regulation of F-actin-dependent processes by the Abl family of tyrosine kinases. *J Cell Sci* 2003; **116**(Pt 13): 2613–2626.
4. Wang JY. Regulation of cell death by the Abl tyrosine kinase. *Oncogene* 2000; **19**: 5643–5650.
5. Wang JY. Nucleo-cytoplasmic communication in apoptotic response to genotoxic and inflammatory stress. *Cell Res* 2005; **15**: 43–48.
6. Baskaran R, Wood LD, Whitaker LL, Canman CE, Morgan SE, Xu Y *et al.* Ataxia telangiectasia mutant protein activates c-Abl tyrosine kinase in response to ionizing radiation. *Nature* 1997; **387**: 516–519.
7. Preyer M, Shu CW, Wang JY. Delayed activation of Bax by DNA damage in embryonic stem cells with knock-in mutations of the Abl nuclear localization signals. *Cell Death Differ* 2007; **14**: 1139–1148.
8. Tang J, Wang JY, Parker LL. Detection of early Abl kinase activation after ionizing radiation by using a peptide biosensor. *Chembiochem* 2012; **13**: 665–673.
9. Agami R, Blandino G, Oren M, Shaul Y. Interaction of c-Abl and p73alpha and their collaboration to induce apoptosis. *Nature* 1999; **399**: 809–813.
10. Gonfloni S, Di Tella L, Caldarola S, Cannata SM, Klinger FG, Di Bartolomeo C *et al.* Inhibition of the c-Abl-TAp63 pathway protects mouse oocytes from chemotherapy-induced death. *Nat Med* 2009; **15**: 1179–1185.
11. Gong JG, Costanzo A, Yang HQ, Melino G, Kaelin WG Jr., Levrero M *et al.* The tyrosine kinase c-Abl regulates p73 in apoptotic response to cisplatin-induced DNA damage. *Nature* 1999; **399**: 806–809.
12. Yuan ZM, Shioya H, Ishiko T, Sun X, Gu J, Huang YY *et al.* p73 is regulated by tyrosine kinase c-Abl in the apoptotic response to DNA damage. *Nature* 1999; **399**: 814–817.
13. Vigneri P, Wang JY. Induction of apoptosis in chronic myelogenous leukemia cells through nuclear entrapment of BCR-ABL tyrosine kinase. *Nat Med* 2001; **7**: 228–234.
14. Tybulewicz VL, Crawford CE, Jackson PK, Bronson RT, Mulligan RC. Neonatal lethality and lymphopenia in mice with a homozygous disruption of the c-abl proto-oncogene. *Cell* 1991; **65**: 1153–1163.
15. Borges HL, Hunton IC, Wang JY. Reduction of apoptosis in Rb-deficient embryos via Abl knockout. *Oncogene* 2007; **26**: 3868–3877.
16. Galanski M. Recent developments in the field of anticancer platinum complexes. *Recent Pat Anticancer Drug Discov* 2006; **1**: 285–295.
17. Kuhlmann MK, Burkhardt G, Kohler H. Insights into potential cellular mechanisms of cisplatin nephrotoxicity and their clinical application. *Nephrol Dial Transplant* 1997; **12**: 2478–2480.
18. Pabla N, Murphy RF, Liu K, Dong Z. The copper transporter Ctr1 contributes to cisplatin uptake by renal tubular cells during cisplatin nephrotoxicity. *Am J Physiol Renal Physiol* 2009; **296**: F505–F511.
19. Pabla N, Dong Z. Cisplatin nephrotoxicity: mechanisms and renoprotective strategies. *Kidney Int* 2008; **73**: 994–1007.
20. Miller RP, Tadagavadi RK, Ramesh G, Reeves WB. Mechanisms of Cisplatin nephrotoxicity. *Toxins (Basel)* 2010; **2**: 2490–2518.
21. Pabla N, Dong G, Jiang M, Huang S, Kumar MV, Messing RO *et al.* Inhibition of PKC delta reduces cisplatin-induced nephrotoxicity without blocking chemotherapeutic efficacy in mouse models of cancer. *J Clin Invest* 2011; **121**: 2709–2722.
22. Koleske AJ, Gifford AM, Scott ML, Nee M, Bronson RT, Miczek KA *et al.* Essential roles for the Abl and Arg tyrosine kinases in neurulation. *Neuron* 1998; **21**: 1259–1272.
23. Jung FF, Bachinsky DR, Tang SS, Zheng G, Diamant D, Haveran L *et al.* Immortalized rat proximal tubule cells produce membrane bound and soluble megalin. *Kidney Int* 1998; **53**: 358–366.
24. Hanigan MH, Devarajan P. Cisplatin nephrotoxicity: molecular mechanisms. *Cancer Ther* 2003; **1**: 47–61.
25. Liu H, Lu ZG, Miki Y, Yoshida K. Protein kinase C delta induces transcription of the TP53 tumor suppressor gene by controlling death-promoting factor Btf in the apoptotic response to DNA damage. *Mol Cell Biol* 2007; **27**: 8480–8491.
26. Momand J, Zambetti GP, Olson DC, George D, Levine AJ. The mdm-2 oncogene product forms a complex with the p53 protein and inhibits p53-mediated transactivation. *Cell* 1992; **69**: 1237–1245.
27. Ashcroft M, Taya Y, Vousden KH. Stress signals utilize multiple pathways to stabilize p53. *Mol Cell Biol* 2000; **20**: 3224–3233.
28. Barak Y, Juven T, Haffner R, Oren M. mdm2 expression is induced by wild type p53 activity. *EMBO J* 1993; **12**: 461–468.
29. Sionov RV, Moallem E, Berger M, Kazaz A, Gerlitz O, Ben-Neriah Y *et al.* c-Abl neutralizes the inhibitory effect of Mdm2 on p53. *J Biol Chem* 1999; **274**: 8371–8374.
30. Goldberg Z, Vogt Sionov R, Berger M, Zwang Y, Perets R, Van Etten RA *et al.* Tyrosine phosphorylation of Mdm2 by c-Abl: implications for p53 regulation. *EMBO J* 2002; **21**: 3715–3727.
31. Yu J, Zhang L, Hwang PM, Kinzler KW, Vogelstein B. PUMA induces the rapid apoptosis of colorectal cancer cells. *Mol Cell* 2001; **7**: 673–682.
32. Yabuki A, Suzuki S, Matsumot M, Kurohmaru M, Hayashi Y, Nishinakagawa H. Staining pattern of the brush border and detection of cytoplasmic granules in the uriniferous tubules of female DBA/2Cr mouse kidney: comparison among various fixations and stains. *J Vet Med Sci* 2001; **63**: 1339–1342.
33. Wei Q, Dong G, Yang T, Megyesi J, Price PM, Dong Z. Activation and involvement of p53 in cisplatin-induced nephrotoxicity. *Am J Physiol Renal Physiol* 2007; **293**: F1282–F1291.
34. Amente S, Zhang J, Lavadera ML, Lania L, Avvedimento EV, Majello B. Myc and PI3K/AKT signaling cooperatively repress FOXO3a-dependent PUMA and GADD45a gene expression. *Nucleic Acids Res* 2011; **39**: 9498–9507.
35. Flores ER, Tsai KY, Crowley D, Sengupta S, Yang A, McKeon F *et al.* p63 and p73 are required for p53-dependent apoptosis in response to DNA damage. *Nature* 2002; **416**: 560–564.
36. Lee SH, Jung YS, Chung JY, Oh AY, Lee SJ, Choi DH *et al.* Novel tumor suppressive function of Smad4 in serum starvation-induced cell death through PAK1-PUMA pathway. *Cell Death Dis* 2011; **2**: e235.
37. Spender LC, Carter MJ, O'Brien DI, Clark LJ, Yu J, Michalak EM *et al.* Transforming growth factor-beta directly induces p53-up-regulated modulator of apoptosis (PUMA) during the rapid induction of apoptosis in Myc-driven B-cell lymphomas. *J Biol Chem* 2013; **288**: 5198–5209.
38. Wang P, Qiu W, Dudgeon C, Liu H, Huang C, Zambetti GP *et al.* PUMA is directly activated by NF-kappaB and contributes to TNF-alpha-induced apoptosis. *Cell Death Differ* 2009; **16**: 1192–1202.
39. Chipuk JE, Kuwana T, Bouchier-Hayes L, Droin NM, Newmeyer DD, Schuler M *et al.* Direct activation of Bax by p53 mediates mitochondrial membrane permeabilization and apoptosis. *Science* 2004; **303**: 1010–1014.
40. Mihara M, Erster S, Zaika A, Petrenko O, Chittenden T, Pancoska P *et al.* p53 has a direct apoptogenic role at the mitochondria. *Mol Cell* 2003; **11**: 577–590.
41. Vaseva AV, Marchenko ND, Ji K, Tsirka SE, Holzmann S, Moll UM. p53 opens the mitochondrial permeability transition pore to trigger necrosis. *Cell* 2012; **149**: 1536–1548.
42. Galluzzi L, Vitale I, Abrams JM, Alnemri ES, Baehrecke EH, Blagosklonny MV *et al.* Molecular definitions of cell death subroutines: recommendations of the Nomenclature Colmmittee on Cell Death 2012. *Cell Death Differ* 2012; **19**: 107–120.
43. Thadhani R, Pascual M, Bonventre JV. Acute renal failure. *N Engl J Med* 1996; **334**: 1448–1460.
44. Vaidya VS, Ferguson MA, Bonventre JV. Biomarkers of acute kidney injury. *Annu Rev Pharmacol Toxicol* 2008; **48**: 463–493.
45. Ichimura T, Bonventre JV, Bailly V, Wei H, Hession CA, Cate RL *et al.* Kidney injury molecule-1 (KIM-1), a putative epithelial cell adhesion molecule containing a novel immunoglobulin domain, is up-regulated in renal cells after injury. *J Biol Chem* 1998; **273**: 4135–4142.
46. Kaur T, Mukherjea D, Sheehan K, Jajoo S, Rybak LP, Ramkumar V. Short interfering RNA against STAT1 attenuates cisplatin-induced ototoxicity in the rat by suppressing inflammation. *Cell Death Dis* 2011; **2**: e180.
47. Kumar S, Bharti A, Mishra NC, Raina D, Kharbanda S, Saxena S *et al.* Targeting of the c-Abl tyrosine kinase to mitochondria in the necrotic cell death response to oxidative stress. *J Biol Chem* 2001; **276**: 17281–17285.
48. Li B, Wang X, Rasheed N, Hu Y, Boast S, Ishii T *et al.* Distinct roles of c-Abl and Atm in oxidative stress response are mediated by protein kinase C delta. *Genes Dev* 2004; **18**: 1824–1837.
49. Vousden KH. Apoptosis. p53 and PUMA: a deadly duo. *Science* 2005; **309**: 1685–1686.
50. Chipuk JE, Green DR. PUMA cooperates with direct activator proteins to promote mitochondrial outer membrane permeabilization and apoptosis. *Cell Cycle* 2009; **8**: 2692–2696.
51. Ming L, Wang P, Bank A, Yu J, Zhang L. PUMA dissociates Bax and Bcl-X(L) to induce apoptosis in colon cancer cells. *J Biol Chem* 2006; **281**: 16034–16042.
52. Strasser A, Cory S, Adams JM. Deciphering the rules of programmed cell death to improve therapy of cancer and other diseases. *EMBO J* 2011; **30**: 3667–3683.
53. Yu J, Zhang L. No PUMA, no death: implications for p53-dependent apoptosis. *Cancer Cell* 2003; **4**: 248–249.
54. Yu J, Zhang L. PUMA, a potent killer with or without p53. *Oncogene* 2008; **27**(Suppl 1): S71–S83.
55. Weiner MW, Jacobs C. Mechanism of cisplatin nephrotoxicity. *Fed Proc* 1983; **42**: 2974–2978.
56. Jacks T, Remington L, Williams BO, Schmitt EM, Halachmi S, Bronson RT *et al.* Tumor spectrum analysis in p53-mutant mice. *Curr Biol* 1994; **4**: 1–7.
57. Wolff NC, Randle DE, Egorin MJ, Minna JD, Ilaria RL Jr. Imatinib mesylate efficiently achieves therapeutic intratumor concentrations *in vivo* but has limited activity in a xenograft model of small cell lung cancer. *Clin Cancer Res* 2004; **10**: 3528–3534.
58. Terryn S, Jouret F, Vandenabeele F, Smolders I, Moreels M, Devuyst O *et al.* A primary culture of mouse proximal tubular cells, established on collagen-coated membranes. *Am J Physiol Renal Physiol* 2007; **293**: F476–F485.

Supplementary Information accompanies this paper on Cell Death and Differentiation website (http://www.nature.com/cdd)